

Supporting information for the article:

Lović, J.D., N.R. Elezović, B.M. Jović, P. Zabinski, L. Gajić-Krstajić, and V.D. Jović. 2018. "Electrodeposited AgPd Alloy Coatings as Efficient Catalysts for the Ethanol Oxidation Reaction." *International Journal of Hydrogen Energy* 43 (39): 18498–508.
<https://doi.org/10.1016/j.ijhydene.2018.08.056>.

Supporting information

Electrodeposited AgPd alloy coatings as efficient catalysts for the ethanol oxidation reaction

J.D. Lović^a, N.R. Elezović^b, B.M. Jović^b, P. Zabinski^c, Lj. Gajić-Krstajić^d, V.D. Jović^b

^a *Institute of Electrochemistry, ICTM, University of Belgrade, 11000 Belgrade, Njegoševa 12, Serbia*

^b *Institute for Multidisciplinary Research University of Belgrade, 11030 Belgrade, Kneza Višeslava 1, Serbia*

^c *AGH University of Science and Technology, Faculty of Non-Ferrous Metals, Al. Mickiewicza 30,30-059 Krakow, Poland*

^d *Institute of Technical Sciences SASA, 11000 Belgrade, Knez Mihajlova 35, Serbia*

Corresponding author: Dr. Nevenka Elezović (N.R. Elezović)

Institut for Multidisciplinary Research

University of Belgrade

Kneza Višeslava 1, 11030 Belgrade, Serbia

Tel. +381 11 3303688; Fax. +381 11 3055289

e-mail: nelezovic@tmf.bg.ac.rs

1. AgPd alloys electrodeposited under the conditions of non-stationary diffusion

Polarization, $j - E$ curves, for the electrodeposition of pure Ag, pure Pd and AgPd alloys onto Au disc electrode, recorded at a sweep rate of 1 mV s^{-1} and RPM = 0 are presented in **Fig. 1S**. Electrodeposition of Pd is characterized with well-defined diffusion limiting current density ($j_L(\text{Pd})$) in the solution containing only PdCl_2 (PdCl_4^{2-} ions), as well as in the solution containing PdCl_2 and AgCl (AgCl_4^{3-}), with that recorded in the presence of AgCl being slightly higher ($j_L(\text{Pd}) = -59.18 \mu\text{A cm}^{-2}$). In the absence of AgCl sharp peak corresponding to the formation of Pd-H is detected at -0.10 V , while in the presence of AgCl such peak doesn't exist, indicating that Pd-H cannot be formed during the AgPd alloy electrodeposition. Electrodeposition of Ag is seen to commence at about -0.11 V being characterized with the sharp increase of current density until the peak at about -0.15 V has been reached. The $j - E$ curve for AgPd alloy electrodeposition practically represents the sum of those for Pd and Ag. The current density values for AgPd alloy electrodeposition are marked in the figure as $j(1) = 3j_L(\text{Pd})$, $j(2) = 5j_L(\text{Pd})$ and $j(3) = 7j_L(\text{Pd})$.

The composition of the AgPd alloy could be calculated from the parameters of each metal electrodeposition. Masses of the electrodeposited Pd (G_{Pd}) and Ag (G_{Ag}) are given as

$$G_{\text{Pd}} = \frac{j_L(\text{Pd})tM_{\text{Pd}}S}{zF} \quad (1)$$

$$G_{\text{Ag}} = \frac{j(\text{Ag})tM_{\text{Ag}}S}{zF} \quad (2)$$

where: $j_L(\text{Pd})$ – diffusion limiting current density for Pd electrodeposition; t – time of electrodeposition; M_{Pd} – molecular weight of Pd; S – electrode surface area; z – number of exchanged electrons; F – Faradays' constant; j_d – current density for AgPd alloy electrodeposition; $j(\text{Ag})$ – current density for Ag electrodeposition ($j(\text{Ag}) = j_d - j_L(\text{Pd})$); M_{Ag} – molecular weight of Ag.

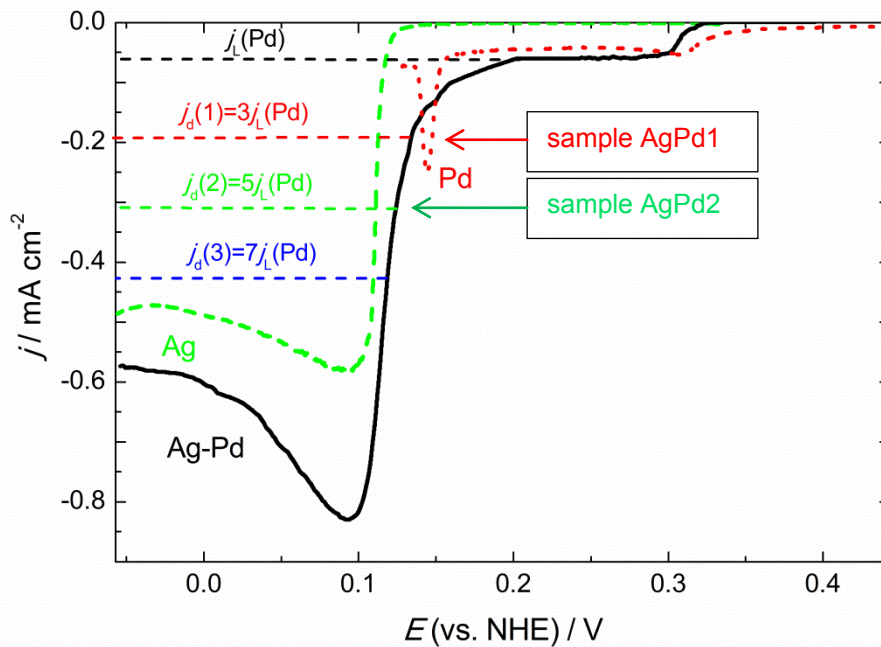


Fig. 1S. The $j - E$ curves for electrodeposition of pure Ag (dashed green line), pure Pd (dotted red line) and AgPd alloy (solid black line), recorded at a sweep rate of 1 mV s^{-1} from the following solutions: (Ag) - $0.04 \text{ M AgCl} + 0.1 \text{ M HCl} + 12 \text{ M LiCl}$; (Pd) - $0.001 \text{ M PdCl}_2 + 0.1 \text{ M HCl} + 12 \text{ M LiCl}$; (AgPd) - $0.001 \text{ M PdCl}_2 + 0.04 \text{ M AgCl} + 0.1 \text{ M HCl} + 12 \text{ M LiCl}$. Current densities for AgPd1 and AgPd2 samples are marked with the arrows.

The composition of the AgPd alloy expressed in mass% of each metal is obtained from the following equations

$$\text{mass\%Pd} = \frac{G_{\text{Pd}}}{G_{\text{Pd}} + G_{\text{Ag}}} \quad (3)$$

$$\text{mass\%Ag} = \frac{G_{\text{Ag}}}{G_{\text{Pd}} + G_{\text{Ag}}} \quad (4)$$

These equations actually represent at.% of metals, since the molecular weights of both metals are very close. Using Eqns. (1-4) the AgPd alloy compositions for different current densities and constant charge ($Q = -0.2 \text{ C cm}^{-2}$) were calculated and presented in **Fig. 2S** as a function of the current density for alloy electrodeposition, j_d (\square , \bullet). As can be seen the content of both metals (at.%) changes exponentially with the increase of current density, starting from $j_L(\text{Pd})$. The amount of Pd decreases, while the amount of Ag increases and already at $j_d = 1.5j_L(\text{Pd})$ equal amounts of Ag and Pd should be electrodeposited.

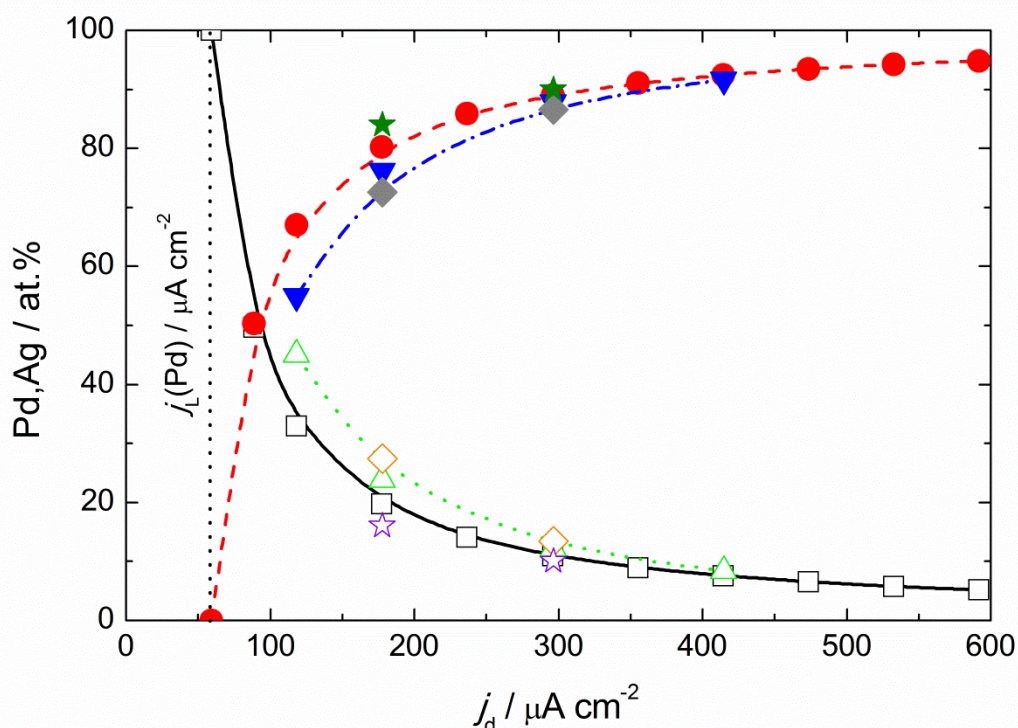


Fig. 2S. Composition of the AgPd alloys calculated from Eqns. (1-4): (\square) at.% Pd; (\bullet) at.% Ag. Composition of AgPd alloys obtained by different techniques: (\triangle) at.% Pd and (∇) at.% Ag obtained from the ALSV; (\diamond) at.% Pd and (\blacklozenge) at.% Ag obtained from the XPS; (\star) at.% Pd and (\blackstar) at.% Ag obtained from the EDS.

2. AgPd alloys electrodeposited under the conditions of convective diffusion

In the case of AgPd alloy electrodeposition in the solution $0.001 \text{ M PdCl}_2 + 0.04 \text{ M AgCl} + 0.1 \text{ M HCl} + 12 \text{ M LiCl}$ the composition cannot be calculated using Eqns. (1-4) since the $j_L(\text{Pd})$ is not well-defined. The current density for Pd electrodeposition increases in the potential range where a plateau is expected, as seen in **Fig. 3S(b)** (black solid line). As in the case of non-stationary diffusion, electrodeposition of Ag commences at the same potential, characterized with the sharp increase of current density. Hence, the alloy composition must be determined by other techniques, such as ALSV, XPS or EDS.

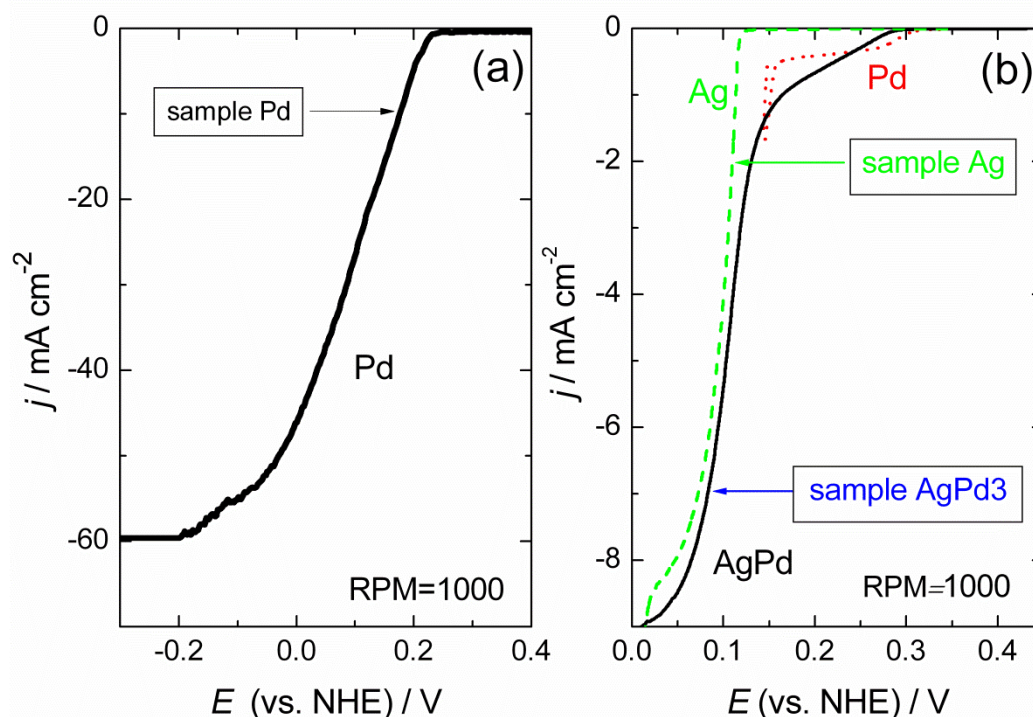


Fig. 3S. (a) The $j - E$ curve for electrodeposition of pure Pd recorded at a sweep rate of 1 mV s^{-1} and RPM=1000 from the solution $0.05 \text{ M PdCl}_2 + 1 \text{ M NH}_4\text{Cl}$. The current density for Pd electrodeposition is marked with the arrow. (b) The $j - E$ curves for electrodeposition of pure Ag (green dashed line), pure Pd (red dotted line) and AgPd alloy (black solid line), recorded at the sweep rate of 1 mV s^{-1} at the RPM=1000 from the following solutions: (Ag) - $0.04 \text{ M AgCl} + 0.1 \text{ M HCl} + 12 \text{ M LiCl}$; (Pd) - $0.001 \text{ M PdCl}_2 + 0.1 \text{ M HCl} + 12 \text{ M LiCl}$; (AgPd) - $0.001 \text{ M PdCl}_2 + 0.04 \text{ M AgCl} + 0.1 \text{ M HCl} + 12 \text{ M LiCl}$. The current densities for Ag and AgPd3 electrodeposition are marked with the arrows.

3. Determination of phases of electrodeposited thin layers of alloys by the anodic linear sweep voltammetry technique (ALSV)

Identification of phases in electrodeposited alloys by x-ray technique is often limited by the size of crystals (lower than 10 nm) appearing on the diffractograms as amorphous and had to be identified by the expensive and often not available transmission electron microscopy (TEM) technique. At the beginning of nineties Jović et al. [1-15] used simple anodic linear sweep voltammetry (ALSV) technique to characterize phase composition of different types of electrodeposited alloys.

The ALSV technique is based on the application of linear sweep voltammetry at low scan rate of 1 mV s^{-1} during the dissolution of thin layer of electrodeposited alloy. Alloys were electrodeposited (up to maximum $10 \text{ }\mu\text{m}$) from the solution containing ions of both metals in one cell and immediately after electrodeposition transferred to another cell (containing electrolyte in which no passivation of any of the metals would take place) for complete dissolution. Concerning the process of the more noble metal electrodeposition/dissolution, two cases can exist in the application of the ALSV technique: (1) the electrodeposition/dissolution process of the more noble metal is reversible. Accordingly, during the dissolution of alloy the ions of the more noble metal must reprecipitate on the spot (since the potential is more negative than the reversible one of the more noble metal); (2) the electrodeposition/dissolution of the more noble metal (or both metals) is irreversible and the dissolution of the more noble component starts at

the potentials more positive than its reversible potential. Accordingly, no reprecipitation of the more noble metal would take place [2].

It was possible to predict the shape of the ALSV of alloys dissolution by consideration of the phase diagram of alloys and the Gibbs energies of phases appearing in the system. Different types of alloys (eutectic [6,10,11], solid solution [4,9], alloys with intermediate phases and/or intermetallic compounds [3,5-8,12-15]) were investigated possessing different shapes of the ALSV responses.

It was discovered that in the case of solid solution type alloys the dissolution can proceed through two separate peaks (AgPd) [1,2,9], or through one peak (CoNi) [1,2,4].

4. Determination of the electrochemically active surface area (EASA) for electrodeposited Pd and AgPd coatings

4.1. EASA of Pd electrode

The procedure of the determination of EASA of Pd electrodes is well-known. Since the charge for the reduction of perfectly flat PdO amounts to $420 \mu\text{C cm}^{-2}$, the EASA for electrodeposited Pd electrode was obtained by dividing the charge under the PdO reduction peak with $420 \mu\text{C cm}^{-2}$. The CVs for electrodeposited Pd electrode in 1 M NaOH, recorded with the sweep rate of 20 mV s^{-1} , are presented in **Fig. 4S**, showing that the cathodic peak for the reduction of PdO increases with increasing anodic potential limit. Potential of the beginning of PdO formation is marked with the arrow (at about -0.160 V), potential region of PdO₂ (and other Pd-oxides) formation is also marked with the arrow in the figure. When the value of E_a reaches 0.544 V the reduction peak of PdO₂ becomes visible on the CV, while the peak of PdO reduction is present on all CVs.

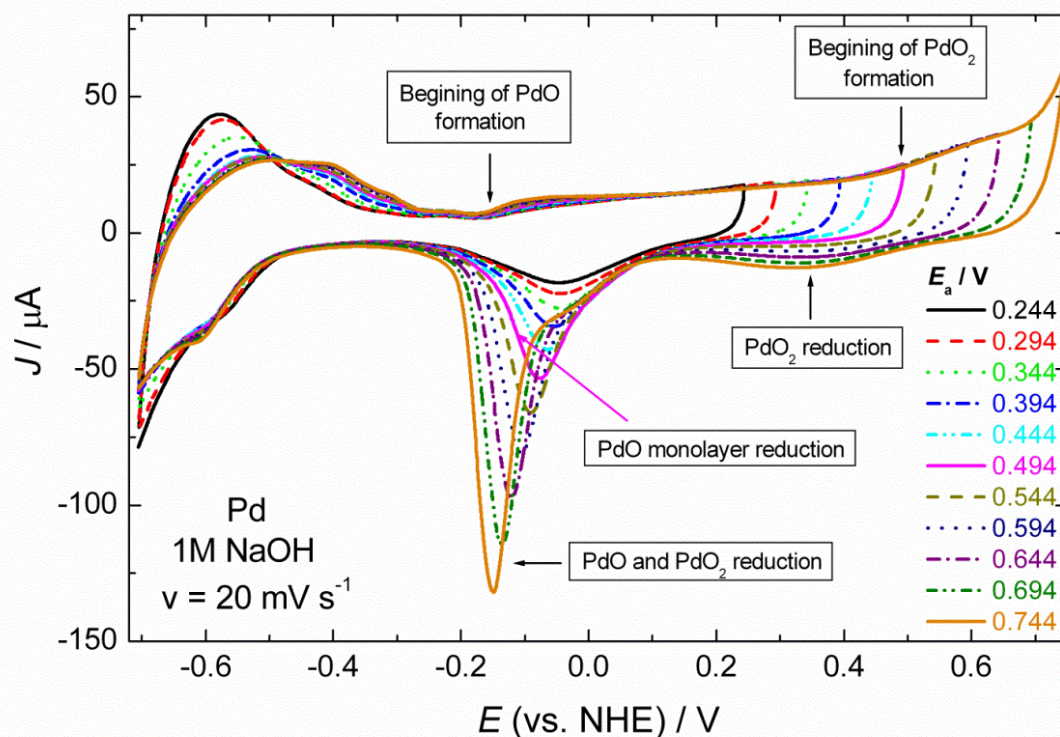


Fig. 4S. CVs for electrodeposited Pd electrode recorded in 1 M NaOH with the sweep rate of 20 mV s^{-1} for different values of the anodic potential limits.

By plotting the charge ($-q$) under the cathodic peak of PdO (and PdO₂) reduction versus anodic potential limit (E_a) it is possible to determine the anodic potential limit for PdO formation, since $-q$ vs. E_a should be characterized by two slopes, one (smaller) corresponding to the reduction of PdO and one (higher) corresponding to the reduction of PdO₂. By the analysis of CVs presented in **Fig. 4S** such dependence was created and presented in **Fig. 5S**. The change of slope appears at $E = 0.494$ V (marked in the figure), indicating that a full monolayer of PdO has been formed at that particular potential. Dividing the charge recorded at $E = 0.494$ V with $420 \mu\text{C cm}^{-2}$ the EASA of Pd sample was found to be 1.13. Linear $-q$ vs. E_a dependence presented in the inset of **Fig. 5S** is obtained by plotting obtained values for charge for the first 6 points. Hence, at the $E_a = 0.494$ V the charge for a PdO monolayer reduction (q_{mon}) amounts to $-478 \mu\text{C cm}^{-2}$ and that particular charge was used for the determination of the EASA for all AgPd alloy samples.

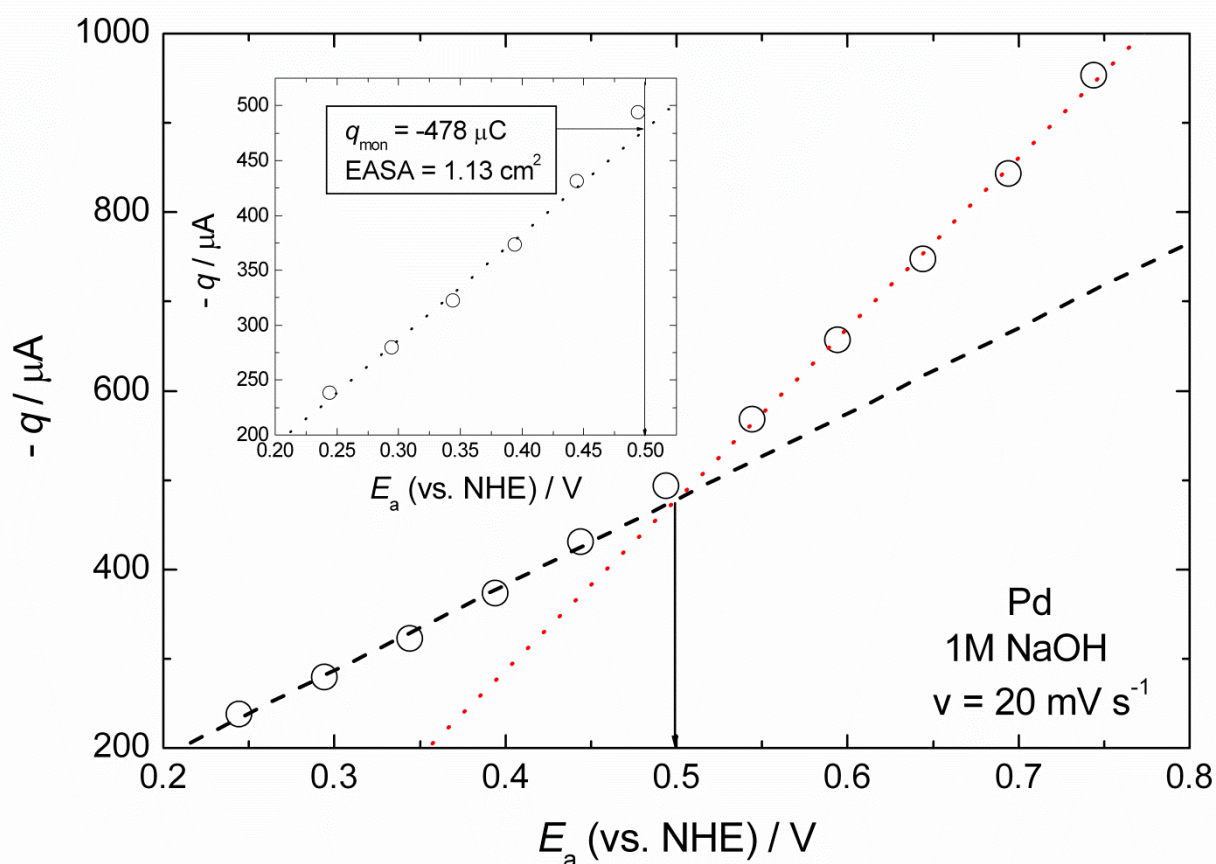


Fig. 5S. $-q$ vs. E_a dependence obtained by the analysis of cathodic charges under the CVs presented in **Fig. 4S**. Inset: dependence of the cathodic charge for PdO reduction as a function of the anodic potential limit.

4.2. EASA of AgPd electrodes

In order to obtain the EASA for electrodeposited AgPd alloy samples the same procedure as that for Pd was applied. Samples were cycled from -0.56 V to different E_a values (starting at 0.294 V and finishing at 0.744 V, with the steps of 0.05 V) with 20 mV s^{-1} and corresponding charges under the cathodic peak of PdO (and PdO₂) reduction were used for EASA determination.

All CVs were of the same shape, the only difference being the peaks current density corresponding to Pd and Ag oxidation and reduction. Typical CVs, recorded for sample AgPd1 are shown in **Fig. 6S**.

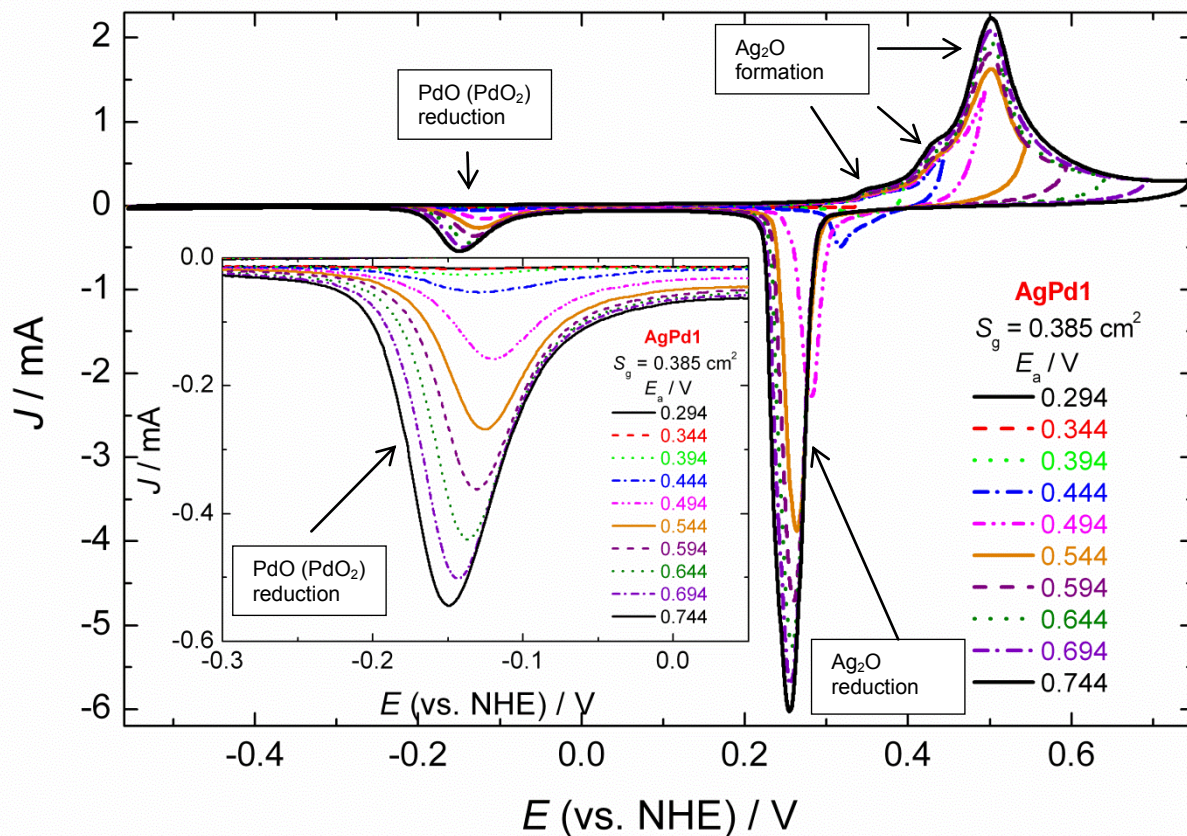


Fig. 6S. Typical CVs recorded for AgPd alloy samples with the sweep rate of 20 mV s^{-1} in the potential range from -0.4 V to 0.5 V. Inset: Peaks of PdO (PdO₂) reduction.

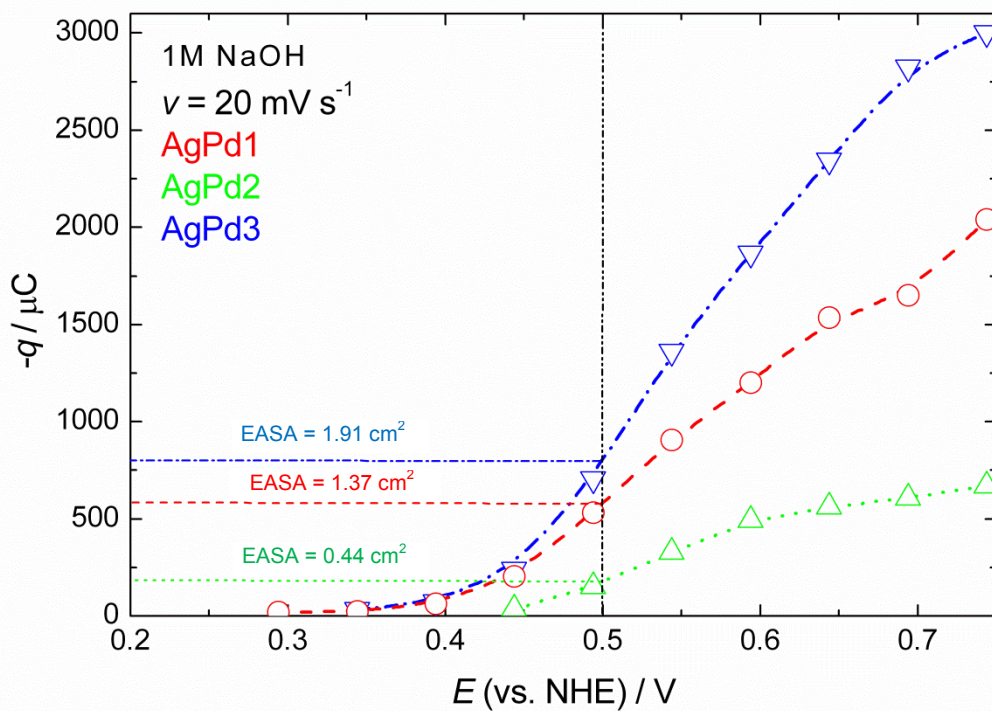


Fig. 7S. $-q$ vs. E_a for all AgPd alloy samples obtained by the integration of the charge under the peak of PdO reduction.

The dependences of q vs. E_a for all AgPd alloy samples differed from that obtained for pure Pd. These dependences are shown in **Fig. 7S**. From the charge obtained at $E_a = 0.494$ V the values of EASA were calculated and given in Table 1 of the paper.

5. XPS analysis of electrodeposited AgPd coatings

As already stated in the paper five peaks, O1s, Ag3d, Pd3d, C1s and Cl2p, were detected on the surfaces of AgPd1, AgPd2 and AgPd3 samples, as shown in **Fig. 8S**.

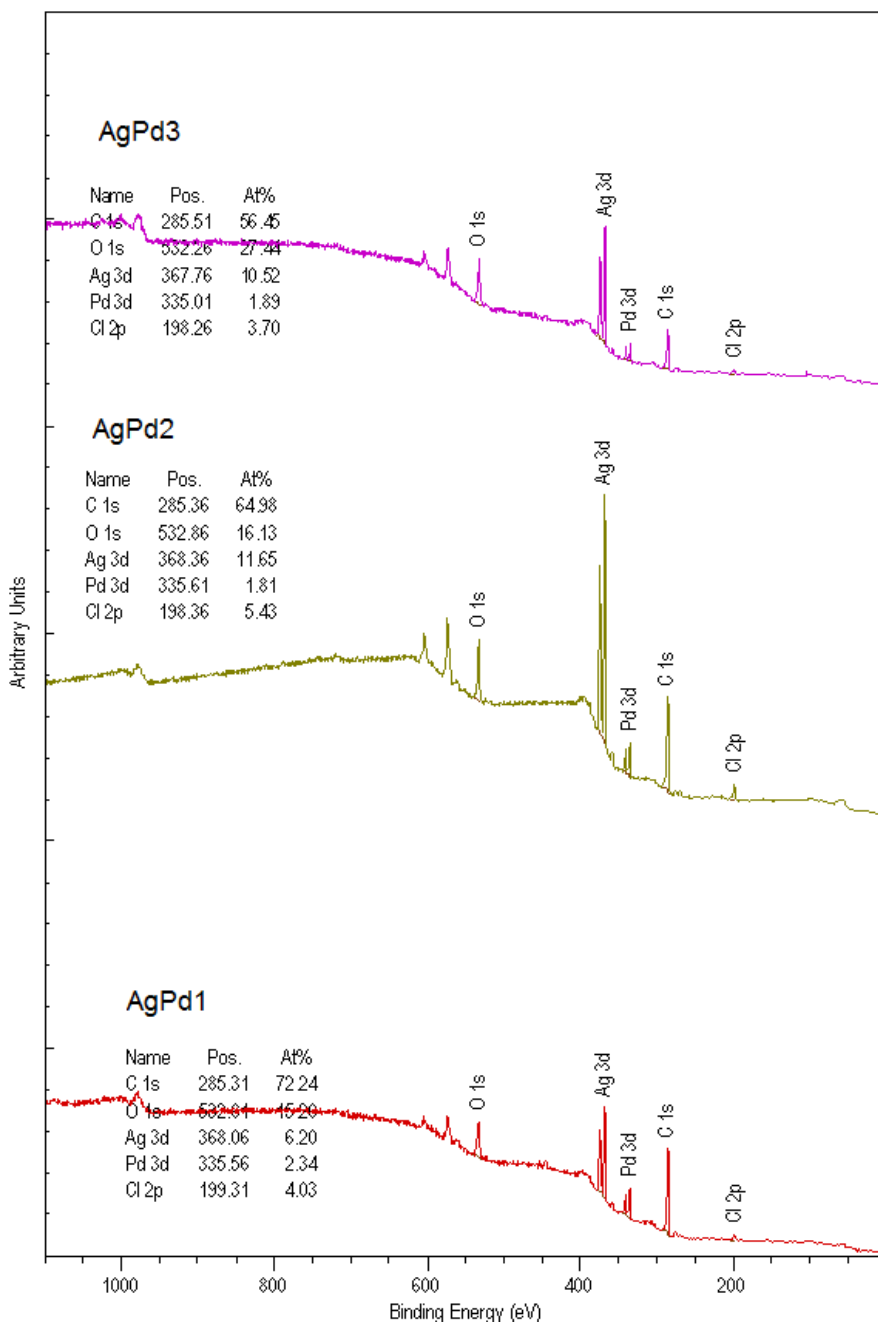


Fig. 8S. XPS spectra for all samples.

6. EDS analysis of electrodeposited AgPd coatings

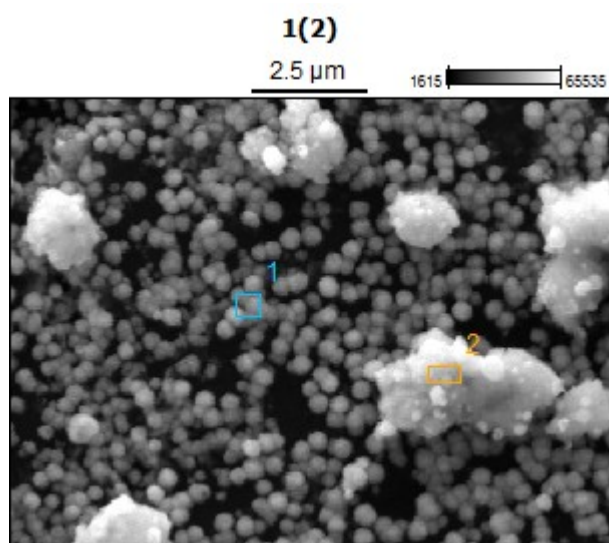


Fig. 9S

Atom %

Table 1S

	C-K	O-K	Al-K	Si-K	P-K	Cl-K	Pd-L	Ag-L
AgPd1-pt1	88.23	0.00	0.20		0.07	0.46	1.89	9.15
AgPd1-pt2	54.87	0.00	0.58	0.18		4.72	0.97	38.69

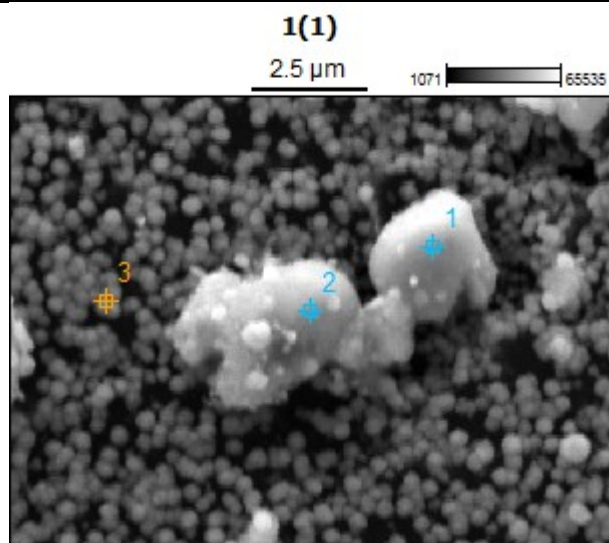


Fig.10S

Atom %

Table 2S

	C-K	O-K	Al-K	Si-K	Cl-K	Pd-L	Ag-L
AgPd1-pt1	38.34	0.00		0.30	7.73	0.98	52.65
AgPd1-pt2	39.62	0.99	0.60		7.41	0.96	50.24
AgPd1-pt3	89.66	0.00	0.18		0.40	1.50	8.26

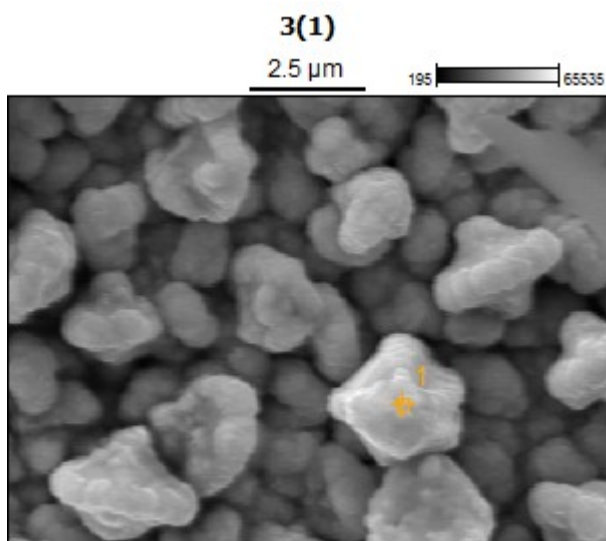


Fig. 11S

Atom %

Table 3S

	<i>C-K</i>	<i>O-K</i>	<i>Al-K</i>	<i>Cl-K</i>	<i>Pd-L</i>	<i>Ag-L</i>
AgPd3-pt1	21.23	16.68	0.76	0.60	2.43	58.24

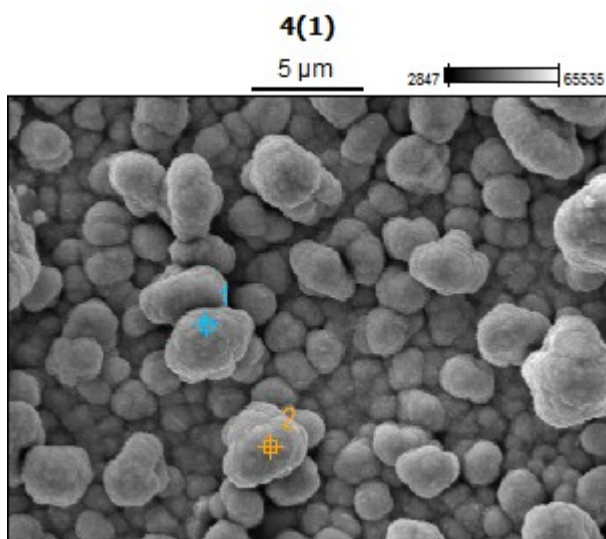


Fig. 12S

Atom %

Table 4S

	<i>C-K</i>	<i>O-K</i>	<i>Si-K</i>	<i>Cl-K</i>	<i>Pd-L</i>	<i>Ag-L</i>
AgPd4-pt1	21.78	5.68	0.40	0.10	7.16	64.88
AgPd4-pt2		1.64		0.15	9.68	88.53

Sample AgPd4 was obtained under the same conditions as sample AgPd3 ($j_d = -7 \text{ mA cm}^{-2}$, RPM = 1000) with the cathodic charge $Q_d = -6 \text{ C cm}^{-2}$.

References

1. A.R. Despić, V.D. Jović, Electrochemical Deposition and Dissolution of Alloys and Metal Composites – Fundamental Aspects, in: R.E. White, J.O'M. Bockris, B.E Conway (Eds.), Modern Aspects of Electrochemistry, Plenum Press, New York, 1995, p.143-232.

2. V.D. Jović, U.Č. Lačnjevac, B.M. Jović, Electrodeposition and Characterization of Alloys and Composite Materials, in: S. Djokić (Eds.), *Modern Aspects of Electrochemistry*, Springer, New York, Heidelberg, Dordrecht, London, 2014, p.1-84.
3. V.D. Jović, N. Tošić, Qualitative and quantitative assessment of phases in electrodeposited Ni + Cd alloys by the ALSV technique, *J. Electroanal. Chem.* 441 (1998) 69-76.
4. V.D. Jović, N. Tošić, M. Stojanović. Characterization of electrodeposited Co + Ni alloys by application of the ALSV technique, *J. Electroanal. Chem.* 420 (1997) 43-51.
5. J. Stevanović, L. Skibina, M. Stefanović, A. Despić, V.D. Jović, Phase-structure analysis of brass by anodic linear-sweep voltammetry, *J. Appl. Electrochem.* 22 (1992) 172-178.
6. V.D. Jović, R.M. Zejnilović, A.R. Despić, J.S. Stevanović, Characterization of electrochemically formed thin layers of binary alloys by linear sweep voltammetry, *J. Appl. Electrochem.* 18 (1988) 511-520.
7. V.D. Jović, A.R. Despić, J.S. Stevanović, S. Spaić, Identification of intermetallic compounds in electrodeposited copper-cadmium alloys by electrochemical techniques *Electrochim. Acta* 34 (1989) 1093-1102.
8. V.D. Jović, S. Spaić, A.R. Despić, J.S. Stevanović, M. Pristavec, Identification of intermetallic compounds in thin layers of electrodeposited Cu–Cd alloys using electrochemical techniques, *Mater. Sci. Technol.* 7 (1991) 1021-1030.
9. V.D. Jović, B.M. Jović, A.R. Despić, Identification of phases in Ag + Pd alloys electrodeposited by the electrochemical technique, *J. Electroanal. Chem.* 357 (1993) 357-372.
10. V.D. Jović, V. Jevtić, The influence of the composition and pH of the electrolyte on the discrimination capacity of the ALSV for the phase structure determination of the alloys, *J. Serb. Chem. Soc.* 61 (1996) 479-493.
11. V.D. Jović, V. Jevtić, Determination of the amount of Zn in electrochemically deposited Zn + Cd alloys by anodic linear sweep voltammetry, *Electrochim. Acta* 43 (1998) 63-68.
12. B.M. Jović, Ts. Dobrovolska, U. Lačnjevac, I. Krastev, V.D. Jović, Characterization of electrodeposited Cd–Co alloy coatings by anodic linear sweep voltammetry, *Electrochim Acta* 54 (2009) 7565-7572.
13. Ts. Dobrovolska, V.D. Jović, B.M. Jović, I. Krastev, Phase identification in electrodeposited Ag–In alloys by ALSV technique, *J. Electroanal. Chem.* 611 (2007) 232-240.
14. Ts. Dobrovolska, I. Krastev, B.M. Jović, V.D. Jović, G. Beck, U. Lačnjevac, A. Zielonka, Phase identification in electrodeposited Ag–Cd alloys by anodic linear sweep voltammetry and X-ray diffraction techniques, *Electrochim. Acta* 56 (2011) 4344-4350.
15. J.S. Stevanović, V.D. Jović, A.R. Despić, Investigation of phase-transformation kinetics in electrodeposited Cu + Cd alloys using anodic linear sweep voltammetry, *J. Electroanal. Chem.* 349 (1993) 365-374.